

Assumed strain finite strip method using the non-periodic B-spline

Hyun-Seok Hong[†] and Kyeong-Ho Kim[†]

Chungbuk Engineering, Structural Div., 57 Karak-dong, Songpa-gu, Seoul, Korea

Chang-Koon Choi[‡]

Department of Civil and Environmental Engineering, KAIST, Daejeon 305-701, Korea

(Received January 12, 2004, Accepted June 26, 2004)

Abstract. An assumed strain finite strip method(FSM) using the non-periodic B-spline for a shell is presented. In the present method, the shape function based on the non-periodic B-splines satisfies the Kronecker delta properties at the boundaries and allows to introduce interior supports in much the same way as in a conventional finite element formulation. In the formulation for a shell, the geometry of the shell is defined by non-periodic B3-splines without any tangential vectors at the ends and the penalty function method is used to incorporate the drilling degrees of freedom. In this study, new assumed strain fields using the non-periodic B-spline function are proposed to overcome the locking problems. The strip formulated in this way does not possess any spurious zero energy modes. The versatility and accuracy of the new approach are demonstrated through a series of numerical examples.

Key words: finite strip; non-periodic B-spline function; assumed strain method.

1. Introduction

The finite strip methods(FSM) are very efficient when used for the analysis of structures which have assemblage of elements with a large dimension in one direction and relatively small dimension in the other direction such as bridges and folded plates. Also the structures to which the FSM can be effectively used are the storage tanks which have large stress gradient in the vertical direction and relatively small stress gradient in the hoop direction.

The semi-analytical finite strip method uses a trigonometric function series which satisfies the end conditions of a strip *a priori* in the longitudinal direction and uses the simple polynomials in the other direction (Cheung 1976). In dealing with problems involving the abrupt changes of shapes, concentrated loading, and internal supports, etc., the second or third derivatives of the functions describing these problems are generally required to be discontinuous. Therefore, the use of trigonometric function series in FSM is disadvantageous since the function series are continuously

[†] Director

[‡] Institute Chair Professor

differentiable. Replacing the trigonometric function series by spline functions, this problem can be overcome since a suitable spline function with the required continuity can be always found (Cheung *et al.* 1983). This method is more flexible than the semi-analytical FSM in treating boundary conditions as only several local splines near the boundary point need to be modified to fit the specified boundary conditions. Recently, Choi and Hong (2001) presented the non-periodic spline FSM for a shell with six degrees of freedom (DOF) per interior node. This method uses the non-periodic B-splines which are modified to have multiple knots at both ends of strip so that the Kronecker delta property is satisfied at boundaries. This concept has been extended to establish the unequally spaced non-periodic spline FSM (Choi *et al.* 2003).

Similar to finite element formulation, when the reduced (or selectively reduced) integration is used in the formulation of the isoparametric spline finite strip method to solve the problems associated with the shear or membrane locking, locking phenomena still remains and a single linear strip cannot remove all the spurious zero energy mode (Cheung 1995). It has been known that the finite element formulation based on the assumed strain methods (Bathe and Dvorkin 1985) has no locking phenomena and does not possess any spurious zero energy modes (Park and Stanley 1986, Jang and Pinsky 1986, Hinton and Huang 1986, Choi and Paik 1994). However, the application of assumed strain concept to the spline FSM formulation has been hardly found in the published literature. The use of B3-spline as the shape function for the assumed strain is not easy since the assumed strain field cannot be defined by only the strain at sampling points within a strip.

In this paper, the assumed strain FSM based on the non-periodic B3-splines is formulated in a similar way to the assumed strain finite element formulation. The proposed finite strip element is applicable to both thin and thick cases and has no zero energy modes. The validity and versatility of the new approach are demonstrated by a series of numerical examples.

2. Non-periodic B-splines

2.1 Spline curves and non-periodic B-splines

The spline curves can be represented in terms of periodic B-spline functions as

$$X(t) = \sum_{i=-1}^{n+1} \phi_{i,k}(t) d_i \quad (1)$$

where $X(t)$ is spline curve and $\phi_{i,k}$ represents the i -th periodic B-spline function of order k . d_i is a set of control points (or parameters) which are curve defining vectors.

The B-spline function can be defined by the recursive form expressed as

$$B_{i,1}(t) = \begin{cases} 1 & \text{for } T_i \leq t \leq T_{i+1} \\ 0 & \text{otherwise} \end{cases} \quad (2)$$

and

$$B_{i,k}(t) = \frac{(t - T_i)}{(T_{i+k-1} - T_i)} B_{i,k-1}(t) + \frac{(T_{i+k} - t)}{(T_{i+k} - T_{i+1})} B_{i+1,k-1}(t) \quad \text{for } k \geq 2 \quad (3)$$

where, (T_i, \dots, T_{i+k}) are the knot vectors. For the sake of convenience, let $\phi_i = B_{i-2,4}$ in the expression hereafter.

By substituting multiple knot values T_i s into Eq. (2) at an end (or boundary), the non-periodic B-spline series can be established. The non-periodic B-splines ϕ_i retain the C^{k-2} continuity property and the partition of unity property, thus these B-splines can also be used as the shape function. Then the extra spans beyond the end knots have all zero lengths and thus the initial and final knots of the strip become multiple knots. In the case of cubic spline, its multiplicity is 4 (Choi *et al.* 2001).

Unlike the uniform (periodic) cubic B3-splines which use the tangential vectors at both ends and $m + 1$ internal knot position vectors (Fig. 1(a)), in the non-periodic B-spline finite strip method, the tangential vectors at both ends are not used and the spline curve is defined by $m + 1$ internal knot position vectors only (Fig. 1(b)). In this paper, the equidistant parametrization scheme with equally spaced knots except at boundaries was used (Choi *et al.* 2003).

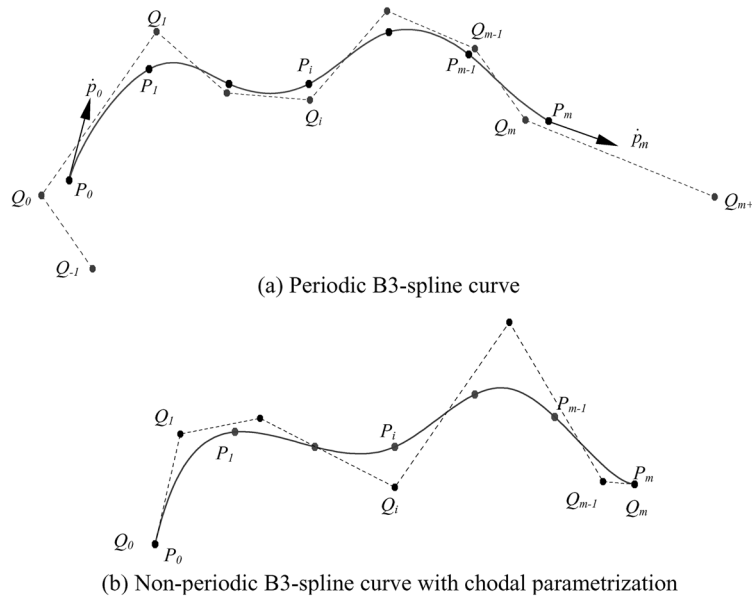


Fig. 1 Spline curves evaluated by two different B3-spline interpolation

2.2 Approximation of spline derivatives

The de Boor algorithm can also be used to compute the derivatives of a B-spline curve recursively (Farin 1992).

$$p^{(j)}(t) = (k-1)(k-2)\dots(k-j) \sum_{i=1}^n d_i^{(j)} \phi_{i,k-j}(t) \tag{4}$$

where

$$d_i^{(j)} = \begin{cases} d_i & j = 0 \\ \frac{d_i^{(j-1)} - d_{i-1}^{(j-1)}}{t_{i+k-j} - t_i} & j > 0 \end{cases} \tag{5}$$

The expression for the first derivative of a B-spline of order k can also be written in terms of two B-spline of the lower order

$$p'(t) = \sum_{i=1}^n \phi_{i,k-1}(t)(k-1) \frac{(d_i - d_{i-1})}{(t_{i+k-1} - t_i)} = \sum_{i=1}^n \phi'_{i,k}(t) d_i \quad (6)$$

where

$$\phi'_{i,k}(t) = (k-1) \left(\frac{\phi_{i,k-1}(t)}{t_{i+k-1} - t_i} - \frac{\phi_{i+1,k-1}(t)}{t_{i+k} - t_{i+1}} \right) \quad (7)$$

Thus, it is shown that the spline family has an additional property that the derivative of B-spline of order k ($\phi'_{i,k}$) can be exactly represented by $\phi_{i,k-1}$ for uniform spacing when the splines are spaced such that their piecewise components are aligned as

$$\phi'_{i,k}(x) = \phi_{i,k-1}(x+m) - \phi_{i,k-1}(x-m) \quad (8)$$

For the sake of convenience, $\phi'_{i,k}$ is centered at $x=0$, and $2m$ is the spacing between consecutive splines for both fields as shown in Eq. (8). Fig. 2 shows the alignment of quadratic (B2) and cubic B-splines (B3) fields, and the ability of the B2-spline to exactly represent the derivative of the B3-spline.

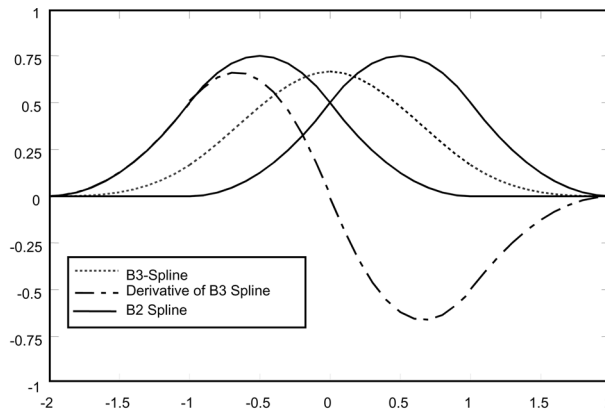


Fig. 2 Spline alignment and derivative approximation

3. Assumed strain formulation of C^0 stress-resultant shell strip

3.1 Definition of geometry and kinematics

The finite strip method is more suitably applied to the structures composed of strip shaped structural elements. A typical finite strip can be generated by dividing an arbitrary shell (plate) into several strips. Each strip is comprised with $(n-1)$ sections (or n interior nodes) and each nodal line between two strips is defined by a curve defining polygon of n vertices (Choi *et al.* 2001). For the

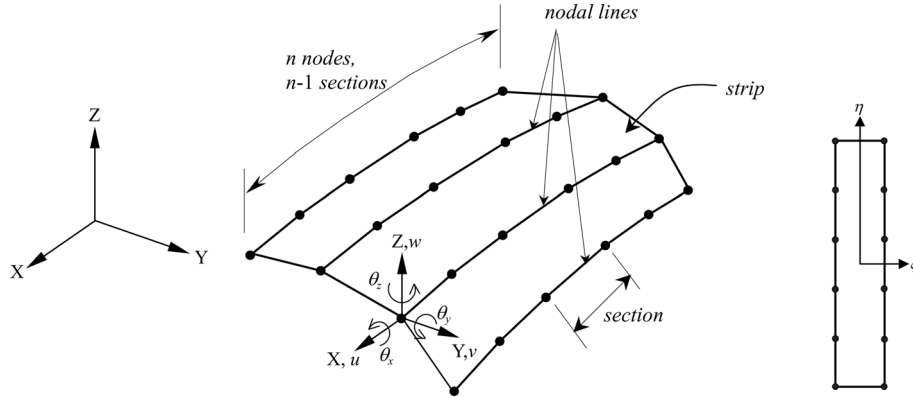


Fig. 3 Strip geometry and isoparametric expression

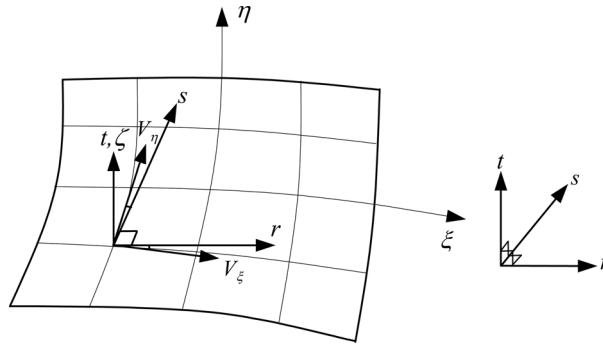


Fig. 4 Local coordinate system at the integration point

resultant stress shell, the independent rotational and translational displacement interpolations are used in the formulation of stiffness matrices and load vectors (Fig. 3).

The mid-surface of the shell is described by two non-dimensional curvilinear coordinates ξ, η and the axis ζ is normal to the shell mid-surface (Fig. 4). Covariant natural unit vectors are defined as follows

$$V_\xi = \frac{1}{A_\xi} \frac{\partial \mathbf{x}}{\partial \xi} = \frac{1}{A_\xi} \begin{Bmatrix} x_{,\xi} \\ y_{,\xi} \\ z_{,\xi} \end{Bmatrix}, \quad V_\eta = \frac{1}{A_\eta} \frac{\partial \mathbf{x}}{\partial \eta} = \frac{1}{A_\eta} \begin{Bmatrix} x_{,\eta} \\ y_{,\eta} \\ z_{,\eta} \end{Bmatrix}, \quad V_\zeta = \frac{1}{A_\zeta} \frac{\partial \mathbf{x}}{\partial \zeta} = \frac{1}{A_\zeta} \begin{Bmatrix} x_{,\zeta} \\ y_{,\zeta} \\ z_{,\zeta} \end{Bmatrix} \quad (9)$$

where

$$A_\xi = |\mathbf{x}_{,\xi}| = (\mathbf{x}_{,\xi} \cdot \mathbf{x}_{,\xi})^{\frac{1}{2}}, \quad A_\eta = |\mathbf{x}_{,\eta}| = (\mathbf{x}_{,\eta} \cdot \mathbf{x}_{,\eta})^{\frac{1}{2}}, \quad A_\zeta = |\mathbf{x}_{,\zeta}| = (\mathbf{x}_{,\zeta} \cdot \mathbf{x}_{,\zeta})^{\frac{1}{2}} \quad (10)$$

The geometry of the C^0 degenerated shell strip is defined in terms of functions of mid-surface as (Kebari *et al.* 1991)

$$\mathbf{x} = \sum_{i=1}^n \sum_{j=1}^2 N_{ij}(\xi, \eta) \mathbf{q}_{ij} + t \mathbf{V}_t \quad (11)$$

where

$$N_{ij}(\xi, \eta) = L_j(\xi) \phi_i(\eta) \quad (12)$$

where \mathbf{V}_t is the unit vector normal to the shell mid-surface at each integration point, t is the linear coordinate in the range $-h/2 < t < h/2$ in the normal direction and h is the thickness at the integration point. $\mathbf{x} = (x, y, z)$ and $\mathbf{q}_{ij} = (x, y, z)_{ij}$ is the i -th curve defining vector of the j -th nodal line of the strip. L_j is the linear Lagrange polynomial and ϕ_i is the non-periodic B3-spline function.

The kinematic variables are interpolated over the mid-surface of strip using two-dimensional interpolations. The displacement vector for a typical point in the shell strip element is introduced as follows

$$\mathbf{u} = \sum_{i=1}^n \sum_{j=1}^2 N_{ij} \tilde{\mathbf{u}}_{ij} + \sum_{i=1}^n \sum_{j=1}^2 N_{ij} \hat{\mathbf{u}}_{ij} \quad (13)$$

where

$$\hat{\mathbf{u}}_{ij} = \begin{Bmatrix} \hat{u}_{ij} \\ \hat{v}_{ij} \\ \hat{w}_{ij} \end{Bmatrix} = \frac{\zeta h}{2} \begin{bmatrix} 0 & n_3 & -m_3 \\ -n_3 & 0 & l_3 \\ m_3 & -l_3 & 0 \end{bmatrix} \begin{Bmatrix} \theta_{xij} \\ \theta_{yij} \\ \theta_{zij} \end{Bmatrix} \quad (14)$$

$\tilde{\mathbf{u}}_{ij}$ denotes the displacement parameter of the shell mid-surface and $\hat{\mathbf{u}}_{ij}$ denotes the displacement parameter of tip of the fiber relative to the mid-surface. It should be noted that these parameters are not physical displacements.

3.2 Definition of covariant strain components

To define the assumed strains in the natural coordinate system, the displacements should be defined also in the natural coordinates. These displacements are referred as the covariant displacements. The covariant displacement components in the natural coordinate system are obtained by projecting the displacement components with respect to the global-Cartesian coordinate system onto the natural coordinate directions (Park *et al.* 1986)

$$u_\xi = \mathbf{V}_\xi \cdot \mathbf{u}, \quad u_\eta = \mathbf{V}_\eta \cdot \mathbf{u}, \quad u_\zeta = \mathbf{V}_\zeta \cdot \mathbf{u} \quad (15)$$

The covariant natural-coordinate unit vectors are then obtained by:

$$\mathbf{V}_\xi = \frac{1}{A_\xi} \frac{\partial \mathbf{x}}{\partial \xi} = \frac{1}{A_\xi} \begin{Bmatrix} x, \xi \\ y, \xi \\ z, \xi \end{Bmatrix}, \quad \mathbf{V}_\eta = \frac{1}{A_\eta} \frac{\partial \mathbf{x}}{\partial \eta} = \frac{1}{A_\eta} \begin{Bmatrix} x, \eta \\ y, \eta \\ z, \eta \end{Bmatrix}, \quad \mathbf{V}_\zeta = \frac{1}{A_\zeta} \frac{\partial \mathbf{x}}{\partial \zeta} = \frac{1}{A_\zeta} \begin{Bmatrix} x, \zeta \\ y, \zeta \\ z, \zeta \end{Bmatrix} \quad (16)$$

where

$$A_\xi = |\mathbf{x}_{,\xi}| = (\mathbf{x}_{,\xi} \cdot \mathbf{x}_{,\xi})^{\frac{1}{2}}, \quad A_\eta = |\mathbf{x}_{,\eta}| = (\mathbf{x}_{,\eta} \cdot \mathbf{x}_{,\eta})^{\frac{1}{2}}, \quad A_\zeta = |\mathbf{x}_{,\zeta}| = (\mathbf{x}_{,\zeta} \cdot \mathbf{x}_{,\zeta})^{\frac{1}{2}} \quad (17)$$

The covariant strains in the natural coordinates are expressed as (Jang *et al.* 1987)

$$\boldsymbol{\varepsilon}_{\xi\xi} = \frac{1}{A_\xi} \frac{\partial u_\xi}{\partial \xi} = \boldsymbol{\varepsilon}_{\xi\xi}^m + \boldsymbol{\varepsilon}_{\xi\xi}^b = \boldsymbol{\varepsilon}_{\xi\xi}^m + z \boldsymbol{\kappa}_{\xi\xi}^b \quad (18a)$$

$$\boldsymbol{\varepsilon}_{\eta\eta} = \frac{1}{A_\eta} \frac{\partial u_\eta}{\partial \eta} = \boldsymbol{\varepsilon}_{\eta\eta}^m + \boldsymbol{\varepsilon}_{\eta\eta}^b = \boldsymbol{\varepsilon}_{\eta\eta}^m + z \boldsymbol{\kappa}_{\eta\eta}^b \quad (18b)$$

$$\boldsymbol{\gamma}_{\xi\eta} = \frac{1}{A_\xi} \frac{\partial u_\eta}{\partial \xi} + \frac{1}{A_\eta} \frac{\partial u_\xi}{\partial \eta} = \boldsymbol{\gamma}_{\xi\eta}^s + z \boldsymbol{\kappa}_{\xi\eta}^b \quad (18c)$$

$$\boldsymbol{\gamma}_{\xi\zeta} = \frac{1}{A_\xi} \frac{\partial u_\zeta}{\partial \xi} + \frac{\partial u_\xi}{\partial \zeta} \quad (18d)$$

$$\boldsymbol{\gamma}_{\eta\zeta} = \frac{1}{A_\eta} \frac{\partial u_\zeta}{\partial \eta} + \frac{\partial u_\eta}{\partial \zeta} \quad (18e)$$

where $z = \zeta h/2$.

The covariant strains can be also expressed by displacement parameters as

$$\bar{\boldsymbol{\varepsilon}}_m = \begin{Bmatrix} \boldsymbol{\varepsilon}_{\xi\xi}^m \\ \boldsymbol{\varepsilon}_{\eta\eta}^m \\ \boldsymbol{\varepsilon}_{\xi\eta}^m \end{Bmatrix} = \begin{Bmatrix} u_{\xi,\xi} \\ u_{\eta,\eta} \\ u_{\xi,\eta} + u_{\eta,\xi} \end{Bmatrix} = \bar{\mathbf{B}}_m \mathbf{a} \quad (19a)$$

$$\bar{\boldsymbol{\varepsilon}}_b = \begin{Bmatrix} \boldsymbol{\kappa}_{\xi\xi}^b \\ \boldsymbol{\kappa}_{\eta\eta}^b \\ \boldsymbol{\kappa}_{\xi\eta}^b \end{Bmatrix} = \begin{Bmatrix} \theta_{\eta,\xi} \\ -\theta_{\xi,\eta} \\ \theta_{\eta,\eta} - \theta_{\xi,\xi} \end{Bmatrix} = \bar{\mathbf{B}}_b \mathbf{a} \quad (19b)$$

$$\bar{\boldsymbol{\varepsilon}}_s = \begin{Bmatrix} \boldsymbol{\gamma}_{\xi\zeta} \\ \boldsymbol{\gamma}_{\eta\zeta} \end{Bmatrix} = \begin{Bmatrix} u_{\zeta,\xi} + \theta_\eta \\ u_{\zeta,\eta} - \theta_\xi \end{Bmatrix} = \bar{\mathbf{B}}_s \mathbf{a} \quad (19c)$$

$$\bar{\boldsymbol{\varepsilon}}_\theta = \theta_\zeta - \frac{1}{2} \left(\frac{\partial u_\xi}{\partial \eta} - \frac{\partial u_\eta}{\partial \xi} \right) = \bar{\mathbf{B}}_\theta \mathbf{a} \quad (19d)$$

where

$$\mathbf{a} = (\mathbf{a}_1, \mathbf{a}_2, \dots, \mathbf{a}_n), \quad \mathbf{a}_i = (\mathbf{u}_i, \boldsymbol{\theta}_i)_g \quad (20a)$$

$$\mathbf{u}_i = (u_i \ v_i \ w_i)^T, \quad \boldsymbol{\theta}_i = (\theta_{xi} \ \theta_{yi} \ \theta_{zi})^T \quad (20b)$$

Displacement-strain matrices of strain matrices are as follows

$$\bar{\mathbf{B}}_m = \begin{bmatrix} \frac{N_{ij,\xi} \mathbf{V}_\xi^T}{A_\xi} & \mathbf{0} \\ \frac{N_{ij,\eta} \mathbf{V}_\eta^T}{A_\eta} & \mathbf{0} \\ \frac{N_{ij,\xi} \mathbf{V}_\eta^T + N_{ij,\eta} \mathbf{V}_\xi^T}{A_\xi} & \mathbf{0} \end{bmatrix}, \quad \bar{\mathbf{B}}_b = \begin{bmatrix} \mathbf{0} & \frac{N_{ij,\xi} \hat{\mathbf{V}}_2^T}{A_\xi} \\ \mathbf{0} & -\frac{N_{ij,\eta} \hat{\mathbf{V}}_1^T}{A_\eta} \\ \mathbf{0} & \frac{N_{ij,\xi} \hat{\mathbf{V}}_1^T - N_{ij,\eta} \hat{\mathbf{V}}_2^T}{A_\eta} \end{bmatrix}, \quad \bar{\mathbf{B}}_s = \begin{bmatrix} \frac{N_{ij,\xi} \mathbf{V}_\zeta^T}{A_\xi} & N_{ij} \hat{\mathbf{V}}_2^T \\ \frac{N_{ij,\eta} \mathbf{V}_\zeta^T}{A_\eta} & -N_{ij} \hat{\mathbf{V}}_1^T \end{bmatrix} \quad (21a-c)$$

$$\bar{\mathbf{B}}_\theta = \left[-\frac{1}{2} \left(\frac{N_{ij,\xi} \mathbf{V}_\eta^T}{A_\xi} - \frac{N_{ij,\eta} \mathbf{V}_\xi^T}{A_\eta} \right) N_{ij} \mathbf{V}_\zeta^T \right] \quad (21d)$$

where

$$\mathbf{V}_\eta \times \mathbf{V}_\zeta = \hat{\mathbf{V}}_1 = \begin{bmatrix} \frac{y,\eta}{A_\eta} z,\zeta - \frac{z,\eta}{A_\eta} y,\zeta \\ \frac{z,\eta}{A_\eta} x,\zeta - \frac{x,\eta}{A_\eta} z,\zeta \\ \frac{x,\eta}{A_\eta} y,\zeta - \frac{y,\eta}{A_\eta} x,\zeta \end{bmatrix} = \begin{bmatrix} \hat{l}_1 \\ \hat{m}_1 \\ \hat{n}_1 \end{bmatrix}, \quad \mathbf{V}_\xi \times \mathbf{V}_\zeta = \hat{\mathbf{V}}_2 = \begin{bmatrix} \frac{z,\xi}{A_\xi} y,\zeta - \frac{y,\xi}{A_\xi} z,\zeta \\ \frac{x,\xi}{A_\xi} z,\zeta - \frac{z,\xi}{A_\xi} x,\zeta \\ \frac{y,\xi}{A_\xi} x,\zeta - \frac{x,\xi}{A_\xi} y,\zeta \end{bmatrix} = \begin{bmatrix} \hat{l}_2 \\ \hat{m}_2 \\ \hat{n}_2 \end{bmatrix} \quad (22)$$

3.3 Assumed covariant strain

3.3.1 Membrane strain

The membrane strains as independent variables are assumed in the natural coordinates as

$$\begin{Bmatrix} \mathcal{E}_{\xi\xi}^m \\ \mathcal{E}_{\eta\eta}^m \\ \mathcal{E}_{\xi\eta}^m \end{Bmatrix} = \sum_{i=1}^n \sum_{j=1}^2 \begin{bmatrix} \frac{N_{ij,\xi} \mathbf{V}_\xi^T}{A_\xi} & \mathbf{0}^T \\ \frac{N_{ij,\eta} \mathbf{V}_\eta^T}{A_\eta} & \mathbf{0}^T \\ \frac{N_{ij,\xi} \mathbf{V}_\eta^T + N_{ij,\eta} \mathbf{V}_\xi^T}{A_\xi} & \mathbf{0}^T \end{bmatrix} \begin{Bmatrix} \mathbf{u}_i \\ \theta_i \end{Bmatrix} \quad (23)$$

where, \mathbf{V}_ξ and \mathbf{V}_η are the unit tangent vectors to the ξ and η axis, respectively.

As shown in Eq. (23), $N_{ij,\xi}$ has constant value along the ξ direction and becomes cubic in the η direction while $N_{ij,\eta}$ is linear in ξ and quadratic in η . Thus the membrane strain $\mathcal{E}_{\xi\xi}^m$ is constant in ξ and cubic in η while the membrane strain $\mathcal{E}_{\eta\eta}^m$ is linear in ξ and quadratic in η . Therefore, the B3-spline function is used for the interpolation of strain $\mathcal{E}_{\xi\xi}^m$ and the B2-spline function for the strain $\mathcal{E}_{\eta\eta}^m$. And the membrane shear strain $\mathcal{E}_{\xi\eta}^m$ may be evaluated by taking the average of strains at the sampling points in the natural coordinates (Jang *et al.* 1987). This can be expressed by Eqs. (24)-(26) as follows

$$\boldsymbol{\varepsilon}_{\xi\xi}^m = \sum_{k=1}^P \Phi_k \tilde{\boldsymbol{\varepsilon}}_{\xi\xi}^m = \sum_{k=1}^P \Phi_k \left(\sum_{i=1}^n \sum_{j=1}^2 \frac{N_{ij,\xi}}{A_\xi} \mathbf{v}_\xi^T \cdot \mathbf{u}_{ij} \right) \quad (24)$$

$$\boldsymbol{\varepsilon}_{\eta\eta}^m = \sum_{k=1}^Q \Psi_k \tilde{\boldsymbol{\varepsilon}}_{\eta\eta}^m = \sum_{k=1}^Q \Psi_k \left(\sum_{i=1}^n \sum_{j=1}^2 \frac{N_{ij,\eta}}{A_\eta} \mathbf{v}_\eta^T \cdot \mathbf{u}_{ij} \right) \quad (25)$$

$$\boldsymbol{\varepsilon}_{\xi\eta}^m = \sum_{k=1}^P \Phi_k \tilde{\boldsymbol{\varepsilon}}_{\xi\eta}^m + \sum_{k=1}^Q \Psi_k \tilde{\boldsymbol{\varepsilon}}_{\eta\xi}^m = \sum_{k=1}^P \Phi_k \left(\sum_{i=1}^n \sum_{j=1}^2 \frac{N_{ij,\xi}}{A_\xi} \mathbf{v}_\eta^T \cdot \mathbf{u}_{ij} \right) + \sum_{k=1}^Q \Psi_k \left(\sum_{i=1}^n \sum_{j=1}^2 \frac{N_{ij,\eta}}{A_\eta} \mathbf{v}_\xi^T \cdot \mathbf{u}_{ij} \right) \quad (26)$$

where

$$\Phi_k = \phi_{k,4}, \quad \Psi_k = \frac{1}{2}(1 - \xi)\phi_{k,3} + \frac{1}{2}(1 + \xi)\phi_{k,3} \quad (27)$$

Table 1 The shape function and sampling points of assumed strain

Interpolation direction and sampling points	Strain component	Interpolation function
<p>Reduced integration point in the transverse direction</p>	$\tilde{\boldsymbol{\varepsilon}}_{\xi\xi}^m, \frac{1}{2}\tilde{\boldsymbol{\varepsilon}}_{\xi\eta}^m$	Φ_1, \dots, Φ_{2n} (B3-spline)
	$\tilde{\gamma}_{\xi\xi}$	
	$\frac{1}{2}\tilde{\boldsymbol{\varepsilon}}_\theta$	
<p>Reduced integration point in the longitudinal direction</p>	$\tilde{\boldsymbol{\varepsilon}}_{\eta\eta}^m, \frac{1}{2}\tilde{\boldsymbol{\varepsilon}}_{\eta\xi}^m$	Ψ_1, \dots, Ψ_{2n} (B2-spline)
	$\tilde{\gamma}_{\eta\xi}$	
	$\frac{1}{2}\tilde{\boldsymbol{\varepsilon}}_\theta$	

• : Given interior node
 × : Strain interpolation points(or sampling points)

and the sampling points P , Q and shape functions Φ_k , Ψ_k for membrane strains are illustrated in Table 1. The terms $\tilde{\epsilon}_{\xi\xi}^m$, $\tilde{\epsilon}_{\eta\eta}^m$ and $\tilde{\epsilon}_{\xi\eta}^m$, $\tilde{\epsilon}_{\eta\xi}^m$ are the membrane strain parameters, which are evaluated at the sampling points. These parameters can be understood as the same parameter d_i used for the definition of the geometry given in Eq. (5).

3.3.2 Shear strain

The assumed shear strain fields are formed by interpolating the strain values at the sampling points which satisfy the Kirchhoff shear constraint condition, i.e., the shear strains $\gamma_{\xi\zeta}$ and $\gamma_{\eta\zeta}$ are equal to zero. Therefore, the following two equations have to be solved:

$$\gamma_{\xi\zeta} = \frac{1}{A_\xi} \frac{\partial u_\zeta}{\partial \xi} + \theta_\eta = 0, \quad \gamma_{\eta\zeta} = \frac{1}{A_\eta} \frac{\partial u_\zeta}{\partial \eta} + \theta_\xi = 0 \quad (28)$$

For linear strip, the polynomial terms in the natural coordinate system for θ_η and $u_{\zeta,\xi}$, and that for θ_ξ and $u_{\zeta,\eta}$ do not match. It is found that the assumed shear strains should be taken as polynomials of at least the following order (Hinton *et al.* 1986).

$$\gamma_{\xi\zeta} = a_1 + a_2\eta + a_3\eta^2 + a_4\eta^3 \quad (29)$$

$$\gamma_{\eta\zeta} = a_5 + a_6\xi + a_7\eta + a_8\xi\eta + a_9\eta^2 + a_{10}\xi\eta^2 \quad (30)$$

If the assumed strain fields are expressed as polynomials of lower order than those in Eqs. (29) and (30), zero energy modes may appear in the strip where the reduced integration is used in the matrix computation.

Similar to the membrane strain, the shear strain $\gamma_{\xi\zeta}$ uses B3-spline in η and $\gamma_{\eta\zeta}$ uses B2-spline in η to construct the shape function of assumed shear strains. Thus, the assumed shear strains can be expressed as

$$\gamma_{\xi\zeta} = \sum_{k=1}^P \Phi_k \tilde{\gamma}_{\xi\zeta} = \sum_{k=1}^P \Phi_k \left\{ \sum_{i=1}^n \sum_{j=1}^2 \left(\frac{N_{ij,\xi}}{A_\xi} \mathbf{V}_\zeta^T \cdot \mathbf{u}_{ij} + N_{ij} \hat{\mathbf{V}}_2^T \cdot \boldsymbol{\theta}_{ij} \right) \right\} \quad (31)$$

$$\gamma_{\eta\zeta} = \sum_{k=1}^Q \Psi_k \tilde{\gamma}_{\eta\zeta} = \sum_{k=1}^Q \Psi_k \left\{ \sum_{i=1}^n \sum_{j=1}^2 \left(\frac{N_{ij,\eta}}{A_\eta} \mathbf{V}_\zeta^T \cdot \mathbf{u}_{ij} - N_{ij} \hat{\mathbf{V}}_1^T \cdot \boldsymbol{\theta}_{ij} \right) \right\} \quad (32)$$

where the sampling points P , Q and shape functions Φ_k , Ψ_k for shear strains are also illustrated in Table 1.

3.3.3 Drilling strain

In order to define the drilling DOF associated with the in-plane rotation of mid-surface, the definition of drilling rotation in continuum mechanics is used as a constraint by the penalty function method in which the drilling DOFs are independent of displacement interpolation (Kebari and Cassell 1991).

$$\epsilon_\theta = \theta_t - 1/2(u_{s,r} - u_{r,s}) = 0 \quad (33)$$

where θ_t is the drilling rotation of shell mid-surface in the local coordinate systems.

The in-plane rotational strains in the natural coordinates are evaluated from the same way as the membrane shear strains which are defined by taking the average of strains at sampling points. The first term of assumed drilling strain uses B2-spline to interpolate along η and the second term uses B3-spline to interpolate along η . The in-plane rotation strains are expressed as Eq. (34). Also, the sampling points and shape functions are illustrated in Table 1.

$$\begin{aligned} \boldsymbol{\varepsilon}_\theta = & \sum_{k=1}^P \Phi_k \left[\sum_{i=1}^n \sum_{j=1}^2 \frac{1}{2} \left(-\frac{N_{ij,\xi}}{A_\xi} \mathbf{V}_\eta^T \mathbf{u}_{ij} + N_{ij} \mathbf{V}_\zeta^T \boldsymbol{\theta}_{ij} \right) \right]_k \\ & + \sum_{k=1}^Q \Psi_k \left[\sum_{i=1}^n \sum_{j=1}^2 \frac{1}{2} \left(\frac{N_{ij,\eta}}{A_\eta} \mathbf{V}_\xi^T \mathbf{u}_i + N_{ij} \mathbf{V}_\zeta^T \boldsymbol{\theta}_{ij} \right) \right]_k \end{aligned} \quad (34)$$

3.4 Local strain of shell

As the assumed strains are expressed by local strains in this study, the natural strains should be transformed into the strains in the local coordinates (Fig. 4). In order to transform the natural strains into the local strains, the relationship between the natural coordinates (ξ, η, ζ) and the local coordinates (r, s, t) should be established as

$$\begin{Bmatrix} u_r \\ u_s \\ u_t \end{Bmatrix} = \mathbf{T}_{sn} \begin{Bmatrix} u_\xi \\ u_\eta \\ u_\zeta \end{Bmatrix} \quad (35)$$

where

$$\mathbf{T}_{sn} = \frac{1}{|\mathbf{V}_\xi \times \mathbf{V}_\eta|} \begin{bmatrix} \mathbf{V}_\eta \cdot \mathbf{V}_s & -\mathbf{V}_\xi \cdot \mathbf{V}_s & 0 \\ -\mathbf{V}_\eta \cdot \mathbf{V}_r & \mathbf{V}_\xi \cdot \mathbf{V}_r & 0 \\ 0 & 0 & |\mathbf{V}_\xi \times \mathbf{V}_\eta| \end{bmatrix} = \begin{bmatrix} t_{r\xi} & t_{r\eta} & 0 \\ t_{s\xi} & t_{s\eta} & 0 \\ 0 & 0 & 1 \end{bmatrix} \quad (36)$$

and where the orthogonal unit vectors $\mathbf{V}_r, \mathbf{V}_s, \mathbf{V}_t$ parallel to the local coordinate axes (r, s, t) are established at each integration point as

$$\mathbf{V}_t = \frac{\mathbf{V}_\xi \times \mathbf{V}_\eta}{|\mathbf{V}_\xi \times \mathbf{V}_\eta|} = \begin{Bmatrix} l_3 \\ m_3 \\ n_3 \end{Bmatrix}, \quad \mathbf{V}_s = \frac{(\mathbf{V}_t \times \mathbf{V}_\xi) + \mathbf{V}_\eta}{|(\mathbf{V}_t \times \mathbf{V}_\xi) + \mathbf{V}_\eta|} = \begin{Bmatrix} l_2 \\ m_2 \\ n_2 \end{Bmatrix}, \quad \mathbf{V}_r = \mathbf{V}_s \times \mathbf{V}_t = \begin{Bmatrix} l_1 \\ m_1 \\ n_1 \end{Bmatrix} \quad (37)$$

and the local strain components are obtained using the following transformation.

$$\begin{bmatrix} \boldsymbol{\varepsilon}_{rr} & \boldsymbol{\varepsilon}_{rs} & \boldsymbol{\varepsilon}_{rt} \\ \boldsymbol{\varepsilon}_{rs} & \boldsymbol{\varepsilon}_{ss} & \boldsymbol{\varepsilon}_{st} \\ \boldsymbol{\varepsilon}_{rt} & \boldsymbol{\varepsilon}_{st} & \boldsymbol{\varepsilon}_{tt} \end{bmatrix} = \mathbf{T}_{sn} \begin{bmatrix} \boldsymbol{\varepsilon}_{\xi\xi} & \boldsymbol{\varepsilon}_{\xi\eta} & \boldsymbol{\varepsilon}_{\xi\zeta} \\ \boldsymbol{\varepsilon}_{\eta\xi} & \boldsymbol{\varepsilon}_{\eta\eta} & \boldsymbol{\varepsilon}_{\eta\zeta} \\ \boldsymbol{\varepsilon}_{\zeta\xi} & \boldsymbol{\varepsilon}_{\zeta\eta} & \boldsymbol{\varepsilon}_{\zeta\zeta} \end{bmatrix} \mathbf{T}_{sn}^T \quad (38)$$

Thus, the local membrane strains, shear strains and in-plane rotational strains are obtained by

following equations.

$$\begin{Bmatrix} \boldsymbol{\varepsilon}_{rr} \\ \boldsymbol{\varepsilon}_{ss} \\ \boldsymbol{\gamma}_{rs} \end{Bmatrix} = \begin{bmatrix} t_{r\xi}^2 & t_{r\eta}^2 & t_{r\xi}t_{r\eta} \\ t_{s\xi}^2 & t_{s\eta}^2 & t_{s\xi}t_{s\eta} \\ 2t_{r\xi}t_{s\xi} & 2t_{r\eta}t_{s\eta} & t_{r\xi}t_{s\eta} + t_{r\eta}t_{s\xi} \end{bmatrix} \begin{Bmatrix} \boldsymbol{\varepsilon}_{\xi\xi} \\ \boldsymbol{\varepsilon}_{\eta\eta} \\ \boldsymbol{\gamma}_{\xi\eta} \end{Bmatrix} \quad (39)$$

$$\begin{Bmatrix} \boldsymbol{\gamma}_{tr} \\ \boldsymbol{\gamma}_{ts} \end{Bmatrix} = \begin{bmatrix} t_{r\xi} & t_{r\eta} \\ t_{s\xi} & t_{s\eta} \end{bmatrix} \begin{Bmatrix} 2\boldsymbol{\varepsilon}_{\xi\zeta} \\ 2\boldsymbol{\varepsilon}_{\eta\zeta} \end{Bmatrix} \quad (40)$$

$$\boldsymbol{\varepsilon}_{\theta}^{local} = (t_{r\xi}t_{s\eta} - t_{s\xi}t_{r\eta})\boldsymbol{\varepsilon}_{\theta}^{natural} \quad (41)$$

3.5 Element stiffness matrix and penalty method

Adopting the conventional explicit integration through the thickness, the generalized strain-displacement relationships for a resultant stress shell strip can be independently established. The membrane stains, shear strains and drilling strains are defined in this study by using the assumed natural stain fields as

$$\boldsymbol{\varepsilon}_m = \begin{Bmatrix} \boldsymbol{\varepsilon}_{rr} \\ \boldsymbol{\varepsilon}_{ss} \\ \boldsymbol{\varepsilon}_{rs} \end{Bmatrix} = \tilde{\mathbf{B}}_m \mathbf{a}, \quad \boldsymbol{\varepsilon}_s = \begin{Bmatrix} \boldsymbol{\gamma}_{tr} \\ \boldsymbol{\gamma}_{ts} \end{Bmatrix} = \tilde{\mathbf{B}}_s \mathbf{a}, \quad \boldsymbol{\varepsilon}_{\theta} = \tilde{\mathbf{B}}_{\theta} \mathbf{a} \quad (42)$$

where, the tilde “~” denotes the terms associated with assumed strains defined in Sec. 3.2 and \mathbf{a} is the displacement parameter as shown in Eq. (20).

While the bending strains are expressed directly by derivatives of displacement parameters as

$$\boldsymbol{\varepsilon}_b = \begin{Bmatrix} \boldsymbol{\kappa}_{rr} \\ \boldsymbol{\kappa}_{ss} \\ \boldsymbol{\kappa}_{rs} \end{Bmatrix} = \begin{Bmatrix} \boldsymbol{\theta}_{s,r} \\ -\boldsymbol{\theta}_{r,s} \\ \boldsymbol{\theta}_{s,s} - \boldsymbol{\theta}_{r,r} \end{Bmatrix} = \mathbf{B}_b \mathbf{a} \quad (43)$$

where

$$\mathbf{B}_b = \begin{bmatrix} \mathbf{0} & N_{ij,r} \mathbf{V}_s^T \\ \mathbf{0} & -N_{ij,s} \mathbf{V}_r^T \\ \mathbf{0} & N_{ij,s} \mathbf{V}_s^T - N_{ij,r} \mathbf{V}_r^T \end{bmatrix} \quad (44)$$

And the stiffness for a shell is derived as

$$\mathbf{K} = \int \tilde{\mathbf{B}}_m^T \mathbf{D}_m \tilde{\mathbf{B}}_m dA + \int \mathbf{B}_b^T \mathbf{D}_b \mathbf{B}_b dA + \int \tilde{\mathbf{B}}_s^T \mathbf{D}_s \tilde{\mathbf{B}}_s dA + \Phi Gh \int \tilde{\mathbf{B}}_{\theta}^T \tilde{\mathbf{B}}_{\theta} dA \quad (45)$$

where, the rigidity matrices \mathbf{D}_m , \mathbf{D}_b , \mathbf{D}_s are associated with membrane, bending and transverse shear strain, respectively, and Φ is the penalty constant. An inappropriate choice of Φ may result in erroneous solution for structures with curved geometry (Chrosielewski *et al.* 1997).

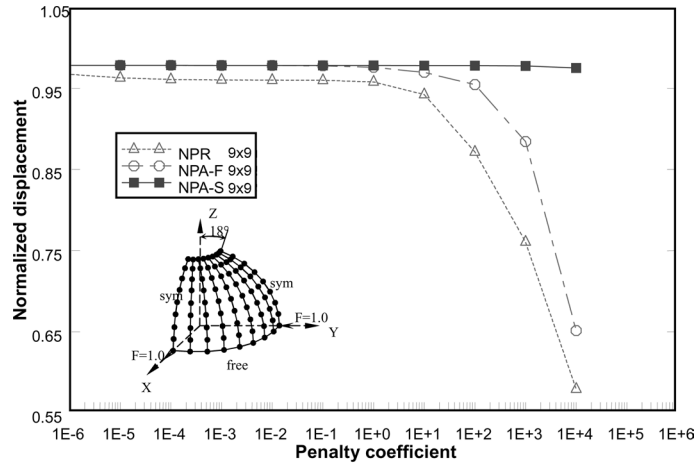


Fig. 5 Influence of penalty coefficients (hemispherical shell)

Table 2 Non-periodic B-spline finite strip element formulated in this study

Strip	Description
NPR	Non-periodic B3-spline shell with reduced integration for shear
NPA-F	Non-periodic B3-spline shell with assumed strains for membrane and shear
NPA-S	Non-periodic B3-spline shell with assumed strains for membrane, shear and drilling

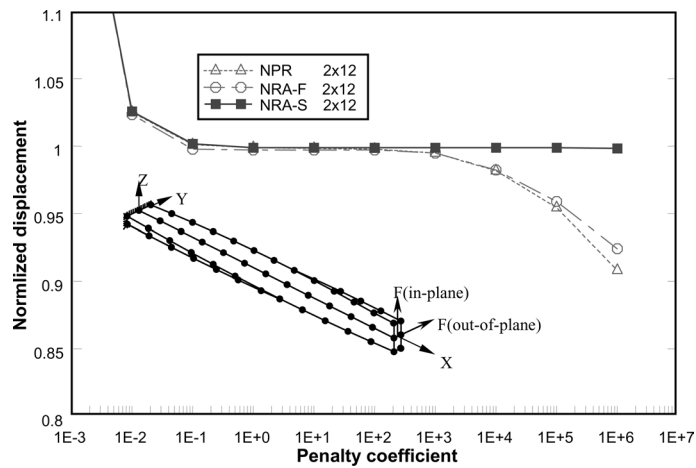


Fig. 6 Influence of penalty coefficients (twisted beam)

Since there is no precise way to determine the value of Φ , an attempt to determine the value of Φ by numerical experiments has been made. The results of a series of tests are shown in Fig. 5. A listing of the linear strips formulated in this study and the abbreviations used to identify them are given in Table 2.

From the results presented in Figs. 5 and 6, it can be seen that for a wide range of acceptable

values of penalty coefficient Φ e.g., $\Phi < 1$ no differences in the solutions are observed for the hemispherical shell. And the basic behaviors are found to be independent of the type of formulation (i.e., NPR, NPA-F, NPA-S). For the higher values of penalty parameter Φ e.g., $\Phi > 1.0$ the calculated displacements and rotations appear to be sensitive to the type of the formulation and only NPA-S shows a perfect independence of penalty parameter. For the twisted beam, the acceptable value of Φ is observed to be from 10^{-1} to 10^2 . Hence, based on the test results of above two cases, Φ is tentatively chosen as 1.0 for the future use in this study.

If the assumed strain method for drilling strain is employed (Eq. (34)), the number of spurious zero energy modes is reduced to one whereas the linear strip element used in this study has 5 spurious zero energy modes when the reduced integration is used. The one remaining zero energy mode can be eliminated by adding the stabilization matrix as the penalty function similar to MacNeal and Harder's method (1988) used in FEM. The energy of the second penalty term used in this study is expressed as

$$\Pi_p = \Phi' Gh \int \varepsilon_p^T \varepsilon_p dA \quad (46)$$

where ε_p is defined by

$$\varepsilon_p = \frac{1}{2n}(\theta_1 + \dots + \theta_n) - \frac{1}{2n}(\theta_{n+1} + \dots + \theta_{2n}) \quad (47)$$

where Φ' is the second penalty coefficient. For the higher values of penalty coefficient Φ' , the membrane locking appears to be more severe and for the lower values of this coefficient, the zero energy modes take place. Based on the numerical experimentation in this study, Φ' is chosen as 10^{-3} , which was also recommended by MacNeal and Harder (1988).

The resulting stiffness matrix of strip formulated by employing the assumed strain method may be expressed as

$$\mathbf{K} = \int \tilde{\mathbf{B}}_m^T \mathbf{D}_m \tilde{\mathbf{B}}_m dA + \int \mathbf{B}_b^T \mathbf{D}_b \mathbf{B}_b dA + \int \tilde{\mathbf{B}}_s^T \mathbf{D}_s \tilde{\mathbf{B}}_s dA + \Phi Gh \int \tilde{\mathbf{B}}_\theta^T \tilde{\mathbf{B}}_\theta dA + \Phi' Gh \int \tilde{\mathbf{B}}_p^T \tilde{\mathbf{B}}_p dA \quad (48)$$

where $\tilde{\mathbf{B}}_p^T$ is derived easily from Eq. (47).

4. Numerical examples

4.1 Integration rule and zero-energy modes

Table 3 gives the integration rule for a linear shell strip used in this study. The integration rule is given as the product of number of Gaussian points in the ξ direction and the corresponding number in the η direction in each section.

As shown in Table 3, the strip designated as NPRa uses the reduced integration for shear and drilling parts in its stiffness matrix calculation while NPRb uses the reduced integration for shear part only. The NPA-F strips adopt the assumed strains for both membrane and shear. The NPA-Fa uses the reduced integration for drilling part and NPA-Fb uses the full (normal) integration for drilling part.

As shown in Table 3, NPRa has a total of 6 spurious zero-energy modes and NPA-Fa has 5.

Table 3 Integration rule and spurious zero energy modes

Strip		Membrane stiffness	Bending stiffness	Shear stiffness	Drilling stiffness	Zero energy modes	Acceptability
Selectively reduced integration	NPRa	2×4	2×4	1×3	1×3	6	×
	NPRb	2×4	2×4	1×3	2×4	1	○
Assumed strain	NPA-Fa	2×4	2×4	2×4	1×3	5	×
	NPA-Fb	2×4	2×4	2×4	2×4	0	○
	NPA-S	2×4	2×4	2×4	2×4	0	○

NPR : a strip with **N**on-**P**eriodic **R**educed integration

NPA : a strip with **N**on-**P**eriodic **A**ssumed strain

-F : a strip with **F**ull Integration for drilling part

Among these spurious modes, five are resulted from under-integration for drilling part and these modes cause singularity problem when the strips are coplanar [19]. On the other hand, strips formulated in this study have almost the same results regardless of integration rule for drilling part. Therefore, NPRb is preferred over NPRa when the reduced integration scheme is used and designated NPR hereafter and NPA-Fb is preferred over NPA-Fa when assumed membrane and shear strain scheme is used and designated as NPA-F in the similar manner.

As shown in Table 3, the zero energy modes do not appear in the case of NPA-F and NPA-S, while NPR has one zero energy mode.

4.2 Shear locking test

For the locking test, a uniformly loaded one half of the symmetric clamped square plate is idealized using 4 strips (Fig. 7). As shown in Fig. 8, there is no locking behavior to appear and the transverse central displacement becomes asymptotic to the Kirchhoff solution for thin plate formulated by the assumed shear field. However, the strip formulated by the reduced integration shows very poor performance as the use of reduced integration for FSM cannot remove the shear locking phenomena in very thin cases.

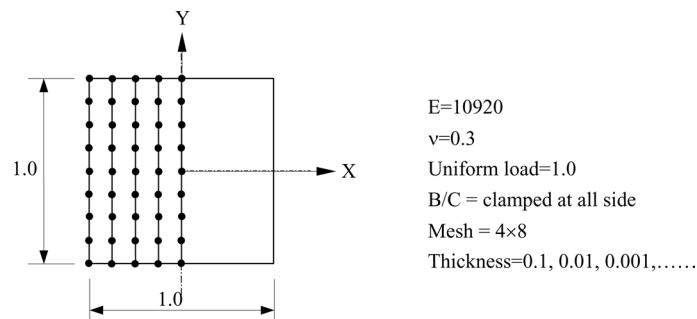


Fig. 7 Uniformly loaded clamped square plate

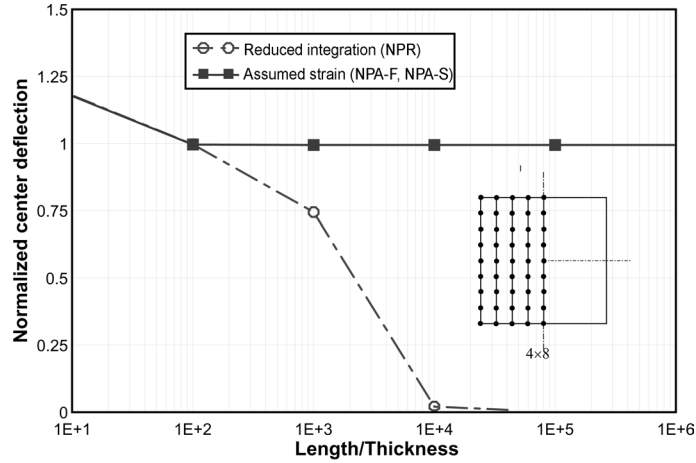


Fig. 8 Shear locking test

4.3 Curved beam

In the problem shown in Fig. 9, the theoretical tip displacements in direction of the load are 0.0873 for in-plane force and 0.5022 for out-of-plane force, respectively. As shown in Table 4, the strip formulated by the reduced integration (NPR) shows inaccurate solution because the reduced integration of a single linear strip creates spurious zero energy modes and the strip formulated by the assumed strain field proposed in this study (NPA-F) shows a good performance.

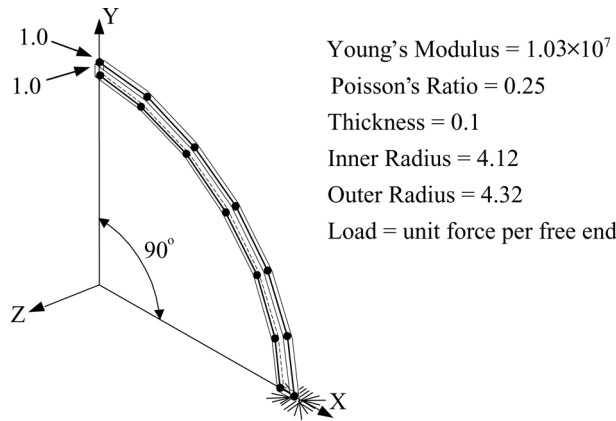


Fig. 9 Curved beam under unit load

Table 4 The displacements in direction of load for curve beam

Loads	FEM		Spline FSM		Theory
	SAP (C&S inc.)	MacNeal (1985)	NPR.	NPA-F	
In-palne	0.0851	0.0727	0.08217	0.08217	0.0873
Out-of-plane	0.4517	0.4776	90.348	0.4857	0.5022

4.4 Hemispherical shell

A hemispherical shell subjected to four radial point loads (two inward and two outward loads) normal to its surface at equal spaces around its equator is known to be very stringent test. Due to the symmetry, only one quadrant of the shell is actually analyzed (Fig. 10). The test checks strip performance for near-inextensible bending of a doubly curved thin shell. This is particularly challenging for a strip which suffers from membrane locking. There is no analytical solution available for this problem, but MacNeal and Harder's result (i.e., 0.094) (1985) is used here as the reference solution for comparison. As shown in Table 5, the membrane locking is observed in the coarse mesh of the reduced integration scheme (NPR), while the assumed strain methods produced much improved results, e.g., an excellent convergence shown by NPA-S.

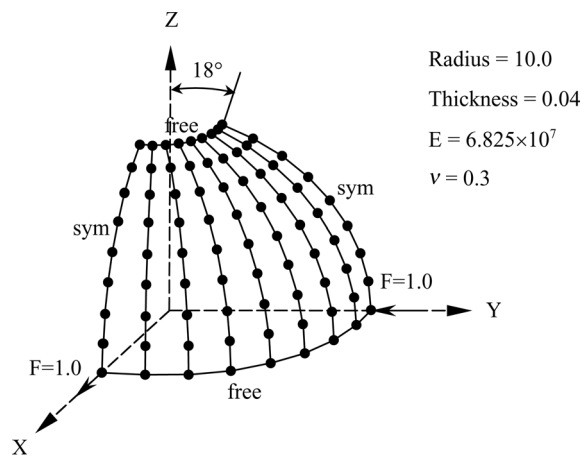


Fig. 10 Hemispherical shell

Table 5 The displacement in direction of load for hemispherical shell

Meshes	FEM				Spline FSM	
	Taylor (1987)	Simo <i>et al.</i> (1989)	Choi <i>et al.</i> (1999)	NPR.	NPA-F	NPA-S
4 × 4	0.08652	0.09337	0.08793	0.02267	0.08874	0.09254
8 × 8	0.09415	0.09281	0.09297	0.09080	0.09261	0.09282
16 × 16	0.09350	0.09291	0.09315	0.09324	0.09368	0.09397

4.5 Twisted beam

This is another test proposed by MacNeal and Harder (1988) to assess the effect of the element warping distortion. A cantilever beam of rectangular cross-section, twisted 90 degrees over its length, is subjected to two concentrated unit loads at its free end as shown in Fig. 11. For the thick beam the analytic solution in the direction of the in-plane load and that of the out-of-plane load are 0.005424 and 0.001754, respectively. The test results by FSM proposed in this study are given in

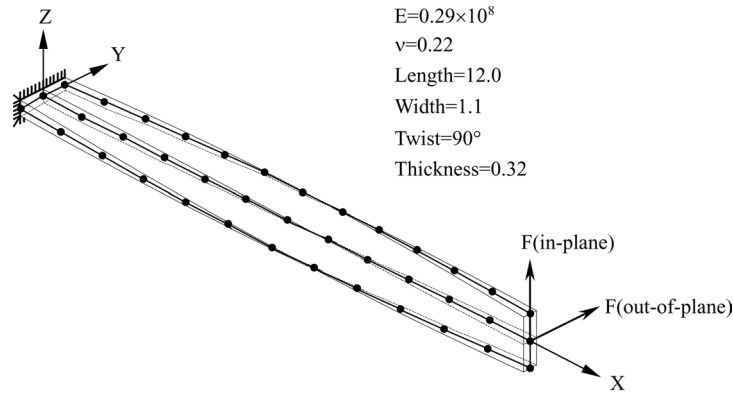
Fig. 11 Twisted beam (2×12)

Table 6 The displacements in direction of load for twisted beam

Loads	Meshes	FEM			Spline FSM		
		Frey (1989)	Taylor (1987)	Choi <i>et al.</i> (1999)	NPR	NPA-F	NPA-S
In-plane	1×6	0.005335	0.005402	0.005391	0.005387	0.005415	0.005319
	2×12	0.005385	0.005410	0.005407	0.005423	0.005417	0.005418
	4×24	0.005397	0.005403	0.005413	0.005418	0.005419	0.005420
Out-of-plane	1×6	0.001719	0.001763	0.001762	0.001718	0.001719	0.001728
	2×12	0.001742	0.001763	0.001758	0.001749	0.001752	0.001752
	4×24	0.001747	0.001751	0.001754	0.001753	0.001754	0.001754

Table 6. All three strips considered here perform well, since they all adopted the same basic geometric definition of the shell as described earlier.

5. Conclusions

A new spline finite strip is formulated by incorporating the assumed strain concept into the non-periodic B-spline FSM of authors' previous study (Choi *et al.* 2001, 2003). The assumed strain fields were used in the finite strip formulation for the membrane, shear, and drilling strains. For the bending strains, the assumed strains are not used because of the violation in the rigid body motion caused by the bending strains. When the assumed strain is used for the drilling strain, the stabilization matrix is needed to be added to eliminate the zero energy modes. Due to the non-availability of precise method to decide the penalty coefficient of stabilization matrix, the penalty coefficient is decided to be 1.0 based on the numerical experimentation that is the only possible way.

For the spline finite strip formulated by the assumed strain fields and by the selectively reduced integration scheme, no shear and membrane locking phenomena and no spurious zero energy modes appeared in NPA-S. Also, NPA-F shows a good performance except the membrane locking phenomena in the coarse mesh of hemispherical shell. However, NPR shows the spurious zero

energy modes in some numerical examples. From the results of standard benchmark analyses, it has been found that the proposed assumed strain based spline finite strip is very accurate and defect-free. The membrane locking is observed for NPR in the coarse mesh of the reduced integration scheme, while the assumed strain methods produced much improved results. It is noted that the assumed strain scheme used in FSM is very effective for the elimination of shear locking as well as membrane locking.

References

- Au, F.T.K. and Cheung, Y.K. (1993), "Isoparametric spline finite strip for plane structures", *Comput. Struct.*, **48**(1), 23-32.
- Bathe, K.J. and Dvorkin, E.N. (1985), "A four-node plate bending element based on Mindlin/Reissner plate theory and a mixed interpolation", *Int. J. Numer. Meth. Eng.*, **21**, 367-383.
- Belytschko, T., Wong, B.L. and Stolarski, H. (1989), "Assumed strain stabilization procedure for the 9-node Lagrange shell element", *Int. J. Numer. Meth. Eng.*, **28**, 385-414.
- Cheung, Y.K. (1976), *The Finite Strip Method in Structural Analysis*, Pergamon, New York.
- Cheung, Y.K. (1983), "Static analysis of right box girder bridges by spline finite strip method", *Proc. of the Institution of Civil Engineers*, Part 2, 75, June, 311-323.
- Cheung, Y.K. and Au, F.T.K. (1995), "Isoparametric spline finite strip for degenerated shells", *Thin-Walled Structures*, **21**, 65-92.
- Choi, C.K. and Paik, J.G. (1994), "An efficient four node degenerated shell element based on the assumed covariant strain", *Struct. Eng. Mech.*, **2**(1), 17-34.
- Choi, C.K., Lee, P.S. and Park, Y.M. (1999), "High performance 4-node flat shell element: NMS-4F element", *Struct. Eng. Mech.*, **8**(2), 209-234.
- Choi, C.K. and Hong, H.S. (2001), "Finite strip analysis of multi-span box girder bridges by using non-periodic B-spline interpolation", *Struct. Eng. Mech.*, **12**(3), 313-328.
- Choi, C.K., Hong, H.S. and Kim, K.H. (2003), "Unequally spaced non-periodic B-spline finite strip method", *Int. J. Numer. Meth. Eng.*, **57**, 35-55.
- Chrosielewski, J., Makowski, J. and Stumpf, H. (1997), "Finite element analysis of smooth, folded and multi-shell structure", *Comput. Meth. Appl. Mech. Eng.*, **141**, 1-46.
- Cook, R.D. (1986), "On the Allman triangle and a related quadrilateral element", *Comput. Struct.*, **22**, 1065-1067.
- Faux, I.D. and Pratt, M.J. (1981), *Computational Geometry for Design and Manufacture*, Ellis Horwood.
- Farin, G. (1992), *Curves and Surfaces for Computer Aided Geometric Design – A Practical Guide*, Academic Press.
- Hinton, E. and Huang, H.C. (1986), "A family of quadrilateral Mindlin plate elements with substitute shear strain fields", *Comput. Struct.*, **23**(3), 409-431.
- Ibrahimbegovic, A., Taylor, R.L. and Wilson, E.L. (1990), "A robust quadrilateral membrane finite element with drilling degree of freedom", *Int. J. Numer. Meth. Eng.*, **30**, 445-457.
- Jang, J. and Pinsky, P.M. (1987), "An assumed covariant strain based 9-node shell element", *Int. J. Numer. Meth. Eng.*, **24**, 2389-2411.
- Jetteur, P. and Frey, F. (1986), "A four node Marguerre element for nonlinear shell analysis", *Engineering Computations*, **3**, 276-282.
- Kebari, H. and Cassell, A.C. (1991), "Non-conforming modes stabilization of a nine-node stress-resultant degenerated shell element with drilling freedom", *Comput. Struct.*, **40**(3), 569-580.
- Li, W.Y., Chueng, Y.K. and Tham, L.G. (1986), "Spline finite strip analysis of general plates", *J. Engng. Mech., ASCE*, **112**(1), 43-54.
- Liu, W.K., Law, E.S., Lam, D. and Belytschko, T. (1986), "Resultant-stress degenerated-shell element", *Comput. Meth. Appl. Mech. Eng.*, **55**, 259-300.
- MacNeal, R.H. and Harder, R.L. (1985), "A proposed standard set of problems to test finite element accuracy", *Finite Elements in Analysis and Design*, **1**, 3-20.

- MacNeal, R.H. and Harder, R.L. (1988), "A refined four-node membrane element with rotational degrees of freedom", *Comput. Struct.*, **28**, 75-84.
- Milford, R.V. and Schnobrich, W.C. (1986), "Degenerated isoparametric finite elements using the explicit integration", *Int. J. Numer. Meth. Eng.*, **23**, 133-154.
- Nukulchai, W.K. (1979), "A simple and efficient finite element for general shell analysis", *Int. J. Numer. Meth. Eng.*, **14**, 179-200.
- Park, K.C. and Stanley, G.M. (1986), "A curved C^0 shell element based on assumed natural-coordinate strains", *J. Appl. Mech.*, ASME, **53**, 279-290.
- Simo, J.C., Fox, D.D. and Rifai, M.S. (1989), "On a stress resultant geometrically exact shell model Part II : The linear theory ; computational aspects", *Comput. Meth. Appl. Mech. Eng.*, **53**, 53-92.
- Taylor, R.L. (1987), "Finite element analysis of linear shell problem", in Whiteman, J.R.(ed.), *Proc. of the Mathematics in Finite Elements and Application*, Academic Press, New York, 191-203.
- Tham, L.G., Li, W.Y. and Cheung, Y.K. (1986), "Bending of skew plates by spline finite strip method", *Comput. Struct.*, **22**(1), 31-38.
- Tham, L.G. (1990), "Application of spline finite strip method in the analysis of space structures", *Thin-Walled Structures*, **10**, 235-246.
- Zienkiewicz, O.C., Taylor, R.L. and Too, J.M. (1971), "Reduced integration technique in general analysis plates and shells", *Int. J. Numer. Meth. Eng.*, **3**, 275-290.
- Zienkiewicz, O.C. (1991), *The Finite Element Method*, McGraw-Hill, fourth edn., **2**, London.

Appendix A

Non-periodic B-spline series

The non-periodic B-splines with n control points can be calculated using the recursive equation and these splines are shown in Fig. A1.

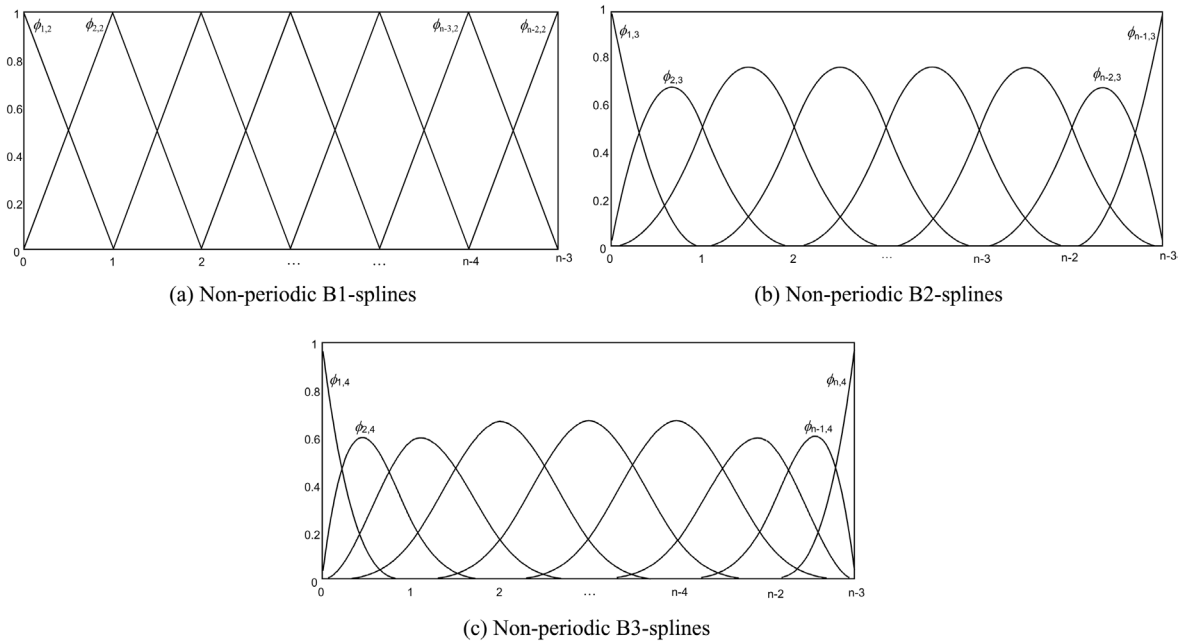


Fig. A1 Non-periodic B-splines with n control points